WIND WAVES AND SWELLS: PROBABILISTIC MODELS FOR DIRECTIONS OF PROPAGATION FOR MOVING SHIPS

ABSTRACT

Samon Ando

Defence Research Establishment Atlantic, P.O. Box 1012, Dartmouth, NS B2Y 3Z7, Canada

Barber and Ursell (1948) measured frequency spectra of ocean waves in order to develop a reliable method of predicting amplitude and period of wind waves and swell from meteorological charts and forecasts. The stroboscopic view of the sea state offered by the series of measured wave spectra at two locations off the east coast of England in their paper provide some useful insights. First, the waves will grow and decay with time at any particular point on the ocean surface. Secondly, the ocean surface is usually covered simultaneously by many wave systems of different nature, but often, predominant systems can be categorized as wind waves and swells. (Wind waves, or a sea, are generated by the wind blowing over a local area of the observer. The swell is generated in a distant storm. So, in general, swell travels in a direction different from that of sea.) Thirdly, the waves are likely to be different at different points on the ocean surface at any time.

So the sea states encountered by a moving ship are constantly changing. Classification societies and navies are concerned about how best to incorporate this fact into the design codes for ships. Researchers, mainly oceanographers, have addressed the question of how the energy of ocean waves is distributed with respect to direction of propagation. For stationary offshore structures, the directional spectrum can be measured at the site. But they have not developed a model that takes into account the relative direction of co-existing sea and swell for moving ships. Such a model is needed to better represent the attributes of a combination of local sea and swell in design wave spectra for ships. The reason is that a ship's behavior in waves is just as sensitive to the direction of oncoming waves relative to the ship's heading as to wave amplitude and period. This paper aims at probability-based characterization of the directions of propagation of sea and swell as encountered by ships operating at sea. Here the direction of sea is assumed to be that of locally-blowing wind. The probability models such as described in this paper are a necessary link between theoretical wave mechanics and practical naval architecture.

Let $\bar{\theta}_w$ and $\bar{\theta}_s$ denote the predominant directions of propagation of wind waves and swell, respectively. We wish to find the conditional probability of $\bar{\theta}_s$ given $\bar{\theta}_w$. Here, we examine a closely equivalent problem of establishing a probability law of the relative angle, say β, of propagation of swell to that of wind wave, where $\beta = \bar{\theta}_s - \bar{\theta}_w$. Questions arise: Can any or all of $\bar{\theta}_w$, $\bar{\theta}_s$, and β be considered random variables taking a value between 0 and 2π? Are the random variables $\bar{\theta}_w$ and $\bar{\theta}_s$ statistically independent of each other? This second question is important because the answer in affirmative represents an enormous simplification of the probabilistic formulation of the problem.

At the moment, the only way to answer these questions is to collect data. This was one of the motivations for us to start compiling the data on winds and waves, among other things, recorded in the logs of Canadian Navy ships. This work is currently in progress [Ando (1999)], but what we have collected so far offers some glimpses of the answers we seek. In this paper, I present some of the results. The data come from the ship logs recorded at every four hours by two Canadian warships over a seven-year period (1969-75) while operating in the areas between North America and Europe, including the North Sea and the Mediterranean. The two ships belonged to different operational

groups, and operated separately both spatially and temporally during the period. It may be pertinent to note that warships of the Canadian Navy typically spend 30 percent of their lives at sea.

Figure 1 shows the scatter diagrams of heights of swell and sea. Notice wide ranges of one variable for a given value of the other. For example, when sea is 5-ft high, swell ranges from 2 ft to 16 ft in Fig. 1a and from 2 ft to 15 ft in Fig. 1b. When swell is 5-ft high, sea ranges from 0 ft to 7 ft in Fig. 1a, and 0 ft to 35 ft in Fig. 1b. It is exactly for this kind of situation where low- and high-frequency waves co-exist that the bimodal wave spectrum of the Ochi-Hubble model is designed.

Figure 2 shows the relative frequencies of $\bar{\theta}_w$ and $\bar{\theta}_s$ (0 deg for wind blowing from due north). The data points in Fig. 1 with zero waveheight are discarded in Fig. 2. The chi-square test suggests that the hypothesis of uniform distribution of $\bar{\theta}_w$ and $\bar{\theta}_s$ between 0 and 2π must be rejected.

Figure 3 shows the relative frequencies of incremental changes, $\bar{\theta}_{w_i} - \bar{\theta}_{w_{i-1}}$ and $\bar{\theta}_{s_i} - \bar{\theta}_{s_{i-1}}$, of the directions of propagation of wind waves and swell between two consecutive observations. The data in this study are indexed in the order of observation. The observations were made every four hours (at the end of a watch) while the ships were steaming during a sortie. The set of observations from one sortie is appended to that from the preceding sortie. The elapsed time between sorties varied from days to months. Figure 3a shows a strong tendency of wind and swell to persist even after four hours. This is somewhat surprising, particularly for seas. For, as Barber and Ursell (1948) conclude, an optimum duration for recording sea states is between 17 and 45 minutes, and in general, the short-term sea spectra are expected to hold for less than two hours. Thus the four-hour period between successive observations in ship logs would be long compared with the memory time of sea states and so each point would be independent of the previous history. In contrast, the degree of persistence is considerably less in Fig. 3b than Fig. 3a. This difference is significant and the cause(s) must be investigated.

Figures 4a and 4b shows the scatter plots of $\bar{\theta}_w$ and $\bar{\theta}_s$ as observed by the two ships. They show surprisingly high degrees of linear correlation (coefficient of correlation between $\bar{\theta}_w$ and $\bar{\theta}_s$ is 0.649 and 0.575 for Figs. 4a and 4b, respectively).

The histograms in Fig. 5 show the distribution of β. They are roughly bell-shaped but highly peaked (coefficient of kurtotis is 3.54 for Fig. 5a and 2.63 for Fig. 5b). The only distribution that fits this condition is the Cauchy distribution,

$$f(x) = \frac{1}{\pi} \frac{c}{c^2 + (x-\mu)^2}, \quad \text{for } -\infty \le x \le \infty, \tag{1}$$

where the constant $c > 0$ is a scale parameter, which controls the shape of the probability density, and the parameter μ locates its center of symmetry. Here the sample space of the random variable is limited, $\beta \in [-\pi, \pi]$, so we need to use the conditional distribution within that space, or the truncated distribution [Ochi (1990)] such that:

$$\begin{aligned} f_*(\beta) &= \frac{f(\beta)}{\int_{-\pi}^{\pi} f(\beta) d\beta}, \quad \text{for } -\pi \le \beta \le \pi, \\ &= 0, \qquad\qquad \text{otherwise,} \end{aligned} \tag{2}$$

where f is given by (1). The curves in Figs. 5a and 5b show the truncated Cauchy distribution (2) with c = 0.32 and 0.36 respectively, and $\mu = 0$ for both, for sample space of $[-\pi, \pi]$. The same probability law agrees well with the actual distributions for both ships, even though the probability laws for the increments for sea and swell, $\bar{\theta}_{w_i} - \bar{\theta}_{w_{i-1}}$ and $\bar{\theta}_{s_i} - \bar{\theta}_{s_{i-1}}$, differ significantly between the two ships, as seen in Fig. 3. This may be construed as an indication of the ergodicity of the process represented by the set $\{\beta_i\}$. Note that although the process represented by the set $\{\beta_i\}$ is rapidly varying and highly

irregular in the time scale on which observations were made, it fails to be a Brownian motion process (or Wiener process), since, for one thing, it does not possess independent increments; see, e.g. Parzen (1962).

So far in this work, $\{\beta_i\}$ has been treated as a process independent of time, so the same probability laws govern it at all times. An interesting, but challenging, possibility is to cast it in the framework of stochastic processes and to develop differential equations that include white noise (approximation of $\bar{\theta}_w$ and $\bar{\theta}_s$) as a driving-force term. Investigation of such a possibility is part of the work currently in progress.

Reference

Ando, S. 1999. "Database for winds, waves, and speeds of CF ships," DREA Tech. Memo., in preparation.

Barber, N.F. and Ursell, F. 1948. "The generation and propagation of ocean waves and swell," *Phil. Trans. Royal Soc. Lond., A,* **240**, 527-560.

Ochi, M.K. 1990. *Applied Probability and Stochastic Processes in Engineering and Physical Sciences*, Wiley.

Parzen, E. 1962. *Stochastic Processes*, Holden-Day.

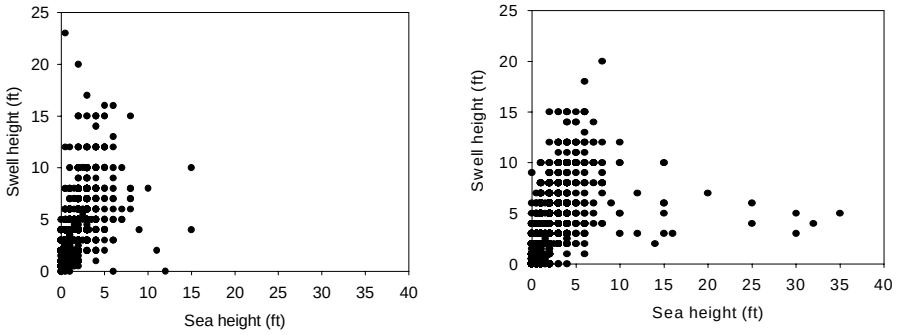

(a) Destroyer A (b) Destroyer B

FIG. 1. Scatter plots of swell heights vs. wind-wave heights as observed every 4 hours by two destroyers at sea between 1969-75: 2596 and 2815 data points for destroyers A and B, respectively. Many data points coincide. Note the difference in maximum sea heights observed by the two ships during the same period.

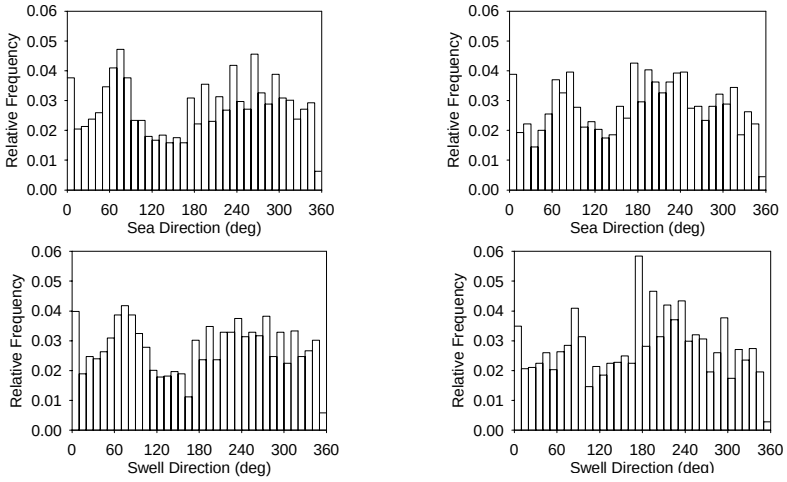

(a) Destroyer A (b) Destroyer B

FIG. 2. Histograms of directions of wind (waves) and swells observed every 4 hours by two destroyers between 1969-75. Only data points for nonzero wave heights in Fig. 1 are taken into account: (a) 2394 data points for sea and 2587 for swell; (b) 2702 data points for sea and 2809 for swell.

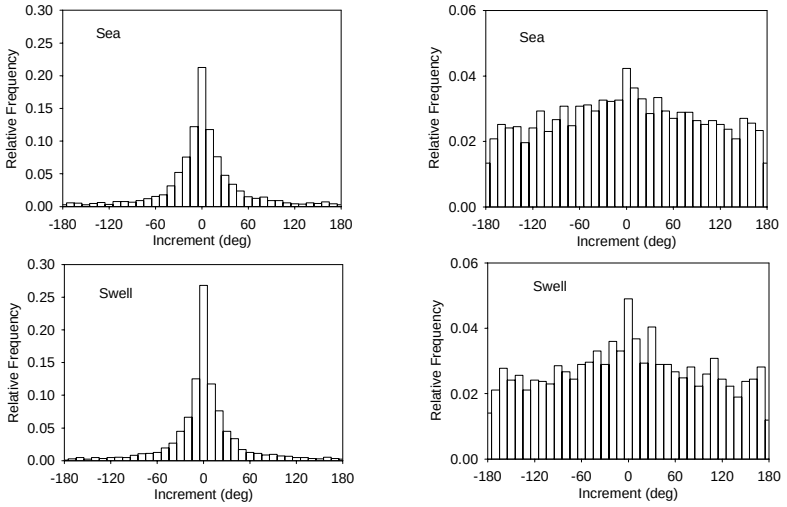

(b) Destroyer B

FIG. 3. Relative frequencies of changes in directions of propagation of sea and swell between successive observations) for the two destroyers. Only data points for nonzero wave heights in Fig. 1 are taken into account: (a) 2394 data points for sea and 2587 for swell; (b) 2702 data points for sea and 2809 for swell.

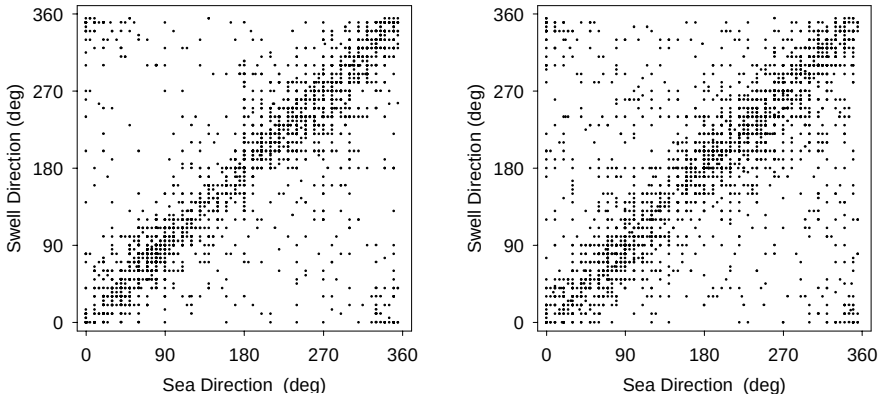

(a) Destroyer A (b) Destroyer B

FIG. 4. Scatter plots of directions of propagation of sea and swells observed every 4 hours by the two destroyers at sea between 1969-75. Only paired data points with nonzero heights for both sea and swell are considered: (a) 2388 data points; (b) 2699 data points.

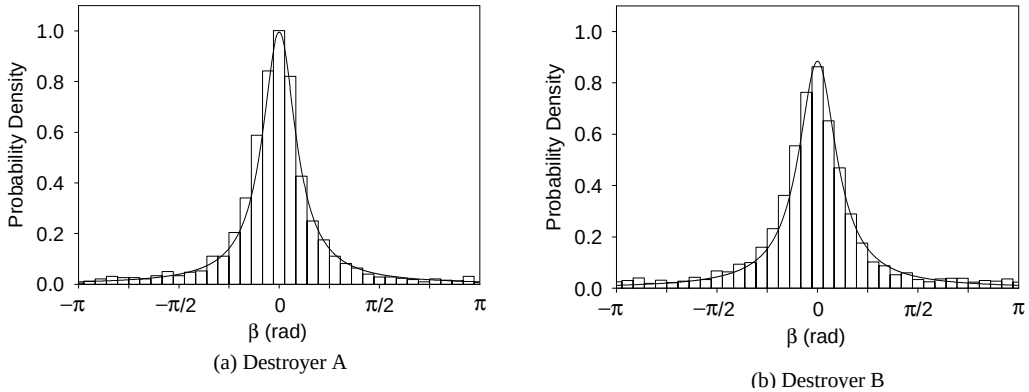

(a) Destroyer A

(b) Destroyer B

FIG. 5. Probability densities of relative angles between directions of propagation of sea and swells observed every 4 hours by two destroyers at sea between 1969-75. Only paired data points with nonzero heights for both sea and swell are considered: (a) 2388 data points; (b) 2699 data points. The histograms are observed distribution and the curves are the fitted truncated Cauchy distribution of equation (2) in the text: $\alpha = 0.32$ for (a) and $\alpha = 0.36$ for (b), and $\mu = 0$ for both.